Academic Journal of Computing & Information Science
ISSN 2616-5775 Vol. 7, Issue 5: 229-235, DOI: 10.25236/AJCIS.2024.070530

Design Optimization Model for Fixed-Sun Mirror Field Based on Monte Carlo Simulation and Particle Swarm Algorithm

Weiyi Zhang[1,*]

[1]*School of Mathematics and Physics, Southwest University of Science and Technology, Mianyang, China*
[*]*Corresponding author: zwy1063208702@outlook.com*

Abstract: *This study focuses on the optimal design of a circular heliostat mirror field, aiming to improve the energy utilization efficiency of a tower solar thermal power plant and help China achieve its carbon emission reduction goals. Parameter analysis and optimization are carried out by tools such as Python and MATLAB, and Monte Carlo simulation and other methods are used to calculate the relevant indexes and establish a constrained optimization model to solve the design problems. For different constraints, the particle swarm algorithm is used to optimize the parameters such as the size of the heliostat mirror and the installation height, so as to maximize the annual average output power per unit mirror area. Ultimately, the optimization model proposed in this study achieves a significant increase in the rated annual output power under different scenarios, which provides an important reference for promoting the application of new energy and achieving the goal of carbon emission reduction.*

Keywords: *Monte Carlo Simulation Methods, Affine Matrix, Particle Swarm Algorithm*

1. Introduction

With the serious threat of global climate change, China is actively responding to the call for emission reduction and promoting the development of new energy sources in order to achieve low-carbon goals [1]. As a key component of the new power system, the design optimization of tower solar photovoltaic power plants is crucial for energy utilization efficiency [2]. This study focuses on the optimal design of a circular heliostat mirror field, which provides design guidance for a solar thermal power plant through parametric analysis and optimization methods with an eye to maximizing optical efficiency and thermal power output. Combining Monte Carlo simulation and particle swarm algorithms, we explore the effects of parameters such as heliostat size and mounting height on the power output, aiming to contribute to China's carbon emission reduction efforts and sustainable development. Through this study, we expect to provide practical suggestions for new energy applications and the realization of carbon neutrality goals.

2. Power generation optimization model

2.1 Introduction to the parameters

The sun's declination δ,

$$sin\,\delta = sin\frac{2\pi D}{365} sin\left(\frac{2\pi}{360}23.45\right) \tag{1}$$

Solar time angle ω,

$$\omega = \frac{\pi}{12}(ST - 12) \tag{2}$$

Solar altitude angle α_s,

$$\sin\alpha_s = \cos\delta\cos\varphi\cos\omega + \sin\delta\sin\varphi \tag{3}$$

Direct solar normalized radiance DNI,

$$DNI = G_0\left[a + b\,exp\left(-\frac{c}{sin\,\alpha_s}\right)\right] \tag{4}$$

$$a = 0.4237 - 0.00821(6 - H)^2 \tag{5}$$

ISSN 2616-5775 Vol. 7, Issue 5: 229-235, DOI: 10.25236/AJCIS.2024.070530

$$b = 0.5055 + 0.00595(6.5 - H)^2 \quad (6)$$

$$c = 0.2711 + 0.01858(2.5 - H)^2 \quad (7)$$

$$E_{field} = DNI \sum_N^i A_i \eta_i \quad (8)$$

Where G_0 is the solar constant, whose value is taken as 1.366 kW/m^2. H is the altitude.

Solar azimuth γ_s,

$$cos\,\gamma_s = \frac{sin\,\delta - sin\,\alpha_s\,sin\,\varphi}{cos\,\alpha_s\,cos\,\varphi} \quad (9)$$

Where φ is the local latitude, and north latitude is positive.

Optical efficiency η,

$$\eta = \eta_{sb}\eta_{cos}\eta_{at}\eta_{trunc}\eta_{ref} \quad (10)$$

Cosine efficiency η_{cos},

$$\eta_{cos} = cos\,\theta \quad (11)$$

Solar transmittance efficiency η_{at},

$$\eta_{at} = 0.99321 - 1.176 \times 10^{-4} d_{HR} + 1.97 \times 10^{-8} d_{HR}^2 \quad (d_{HR} \le 1000m) \quad (12)$$

Truncation efficiency η_{trunc},

$$\eta_{trunc} = \frac{Energy\ received\ by\ the\ collector}{Specular\ total\ reflection\ energy - Shadow\ blocking\ loss\ energy} \quad (13)$$

2.2 Modeling

2.2.1 Arrangement of the fixed-heaven mirror field

From the parameter settings of the heliostat field and the coordinates of the heliostat, we derive the arrangement of its heliostat field as shown in Figure 1.

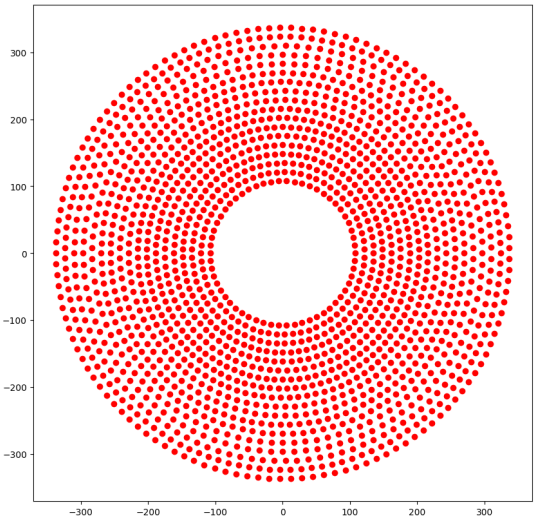

Figure 1: Arrangement of the heliostat field

2.2.2 Monte Carlo simulation method

(1) Firstly, we get the geographic location, time, heliostat and other parameters of the tower optical hotspot station, which is the object of simulation, according to public

Equations. (1)-(13) to model the simulation and calculate the energy output of the plant according to Equations. (4)-(9).

(2) Establish the ground rectangular coordinate system OXYZ with the bottom of the collector as the origin.

(3) The coordinates of the position of the center of the heliostat are chosen to be, and its focus point

ISSN 2616-5775 Vol. 7, Issue 5: 229-235, DOI: 10.25236/AJCIS.2024.070530

is the center of the collector$Q$ $(0,0,H)$. And from the local time and other conditions to calculate the sun's altitude angle, azimuth angle, so as to calculate the direction of the sun's incident light vector for:

$$l_{in} = (\sin(\alpha_s)\cos(\gamma_s), \cos(\alpha_s)\cos(\gamma_s), -\sin(\gamma_s)) \tag{14}$$

And from the coordinates of the reflection point and the focusing point, the direction vector of the reflected ray is calculated as.

$$l_{re} = \frac{Q-M}{|Q-M|} = \frac{(-x_M,-y_M,H-z_M)}{\sqrt{x_M^2+y_M^2+(H-z_M)^2}} \tag{15}$$

Based on the law of reflection of mirrors, the normal vector of the mirror of this fixed-sun mirror is calculated to be:

$$l_{nor} = \frac{l_{re}-l_{in}}{|l_{re}-l_{in}|} \tag{16}$$

(4) The cosine loss and atmospheric transmission efficiency of the heliostat are calculated from Equations. (11)-(12).

(5) The Monte Carlo simulation method is used to calculate the shadow masking efficiency [3]. Firstly, the point P is randomly generated on the mirror surface of the fixed-heaven mirror 1, and the number of points P is n_P , and the coordinates of the point P in the mirror coordinate system are (x_P,$Mirnor$,y_P,$Mirror$,0), and the affine matrix is obtained by the transformation relationship between the mirror coordinate system and the ground coordinate system, so that the coordinates of the point in the ground coordinate system can be calculated as (x_P, y_P, z_P). The coordinates of the point in the ground coordinate system are calculated as (x_P, y_P, z_P). The relationship between the two is:

$$\begin{bmatrix} x_p \\ y_p \\ z_p \end{bmatrix} = \begin{bmatrix} \frac{l_{\mathbf{nor}}(z)}{\sqrt{l_{\mathbf{nor}}(x)^2+l_{\mathbf{nor}}(z)^2}} & \frac{-l_{\mathbf{nor}}(x)\cdot l_{\mathbf{nor}}(y)}{\sqrt{l_{\mathbf{nor}}(x)^2+l_{\mathbf{nor}}(z)^2}} & l_{\mathbf{nor}}(x) \\ 0 & \sqrt{l_{\mathbf{nor}}(x)^2 + l_{\mathbf{nor}}(z)^2} & l_{\mathbf{nor}}(y) \\ \frac{-l_{\mathbf{nor}}(x)}{\sqrt{l_{\mathbf{nor}}(x)^2+l_{\mathbf{nor}}(z)^2}} & \frac{-l_{\mathbf{nor}}(y)\cdot l_{\mathbf{nor}}(z)}{\sqrt{l_{\mathbf{nor}}(x)^2+l_{\mathbf{nor}}(z)^2}} & l_{\mathbf{nor}}(z) \end{bmatrix} \cdot \begin{bmatrix} x_{P,\mathbf{Mirror}} \\ y_{P,\mathbf{Mirror}} \\ z_{P,\mathbf{Mirror}} \end{bmatrix} + \begin{bmatrix} x_M \\ y_M \\ z_M \end{bmatrix} \tag{17}$$

And due to the limitation of the mirror size, the point P satisfies the following conditions.

Then the equation of the incident ray passing through point P in the ground coordinate system with direction vector l_{in} can be calculated as,

$$\frac{x-x_p}{l_{in}(x)} = \frac{y-y_p}{l_{in}(y)} = \frac{z-z_p}{l_{in}(z)} \tag{18}$$

Similarly, the equation of the reflected ray after reflection through this mirror is.

$$\frac{x-x_p}{l_{re}(x)} = \frac{y-y_p}{l_{re}(y)} = \frac{z-z_p}{l_{re}(z)} \tag{19}$$

The shading efficiency is calculated by determining the number of points of intersection of incident and reflected light with the heliostat 2 to see if the light will be blocked.

The specific calculation process is as follows: the normal vector of the heliostat 2 is l_{nor} The coordinates of the center of the mirror are, then the mirror equation is written through the point normal equation:

$$l_{nor}(x_{i-1}) \cdot \left(x - x_{M_{t-1}}\right) + l_{nor}(y_{t-1}) \cdot \left(y - y_{M_{t-1}}\right) + l_{nor}(z_{i-1}) \cdot \left(z - z_{M_{t-1}}\right) = 0 \tag{20}$$

Associated with the above equation, the intersection of incident and reflected rays and the plane of the heliostat 2 is located in the space plane, the coordinates of the intersection point is to the ground as the coordinate system, and then through the (14)-(17) to calculate the coordinates of the intersection point under the coordinate system of the mirror 2 and according to the conditions of the (20) to determine whether the point is within the mirror 2. The number of points of intersection of the incident and reflected rays with the mirror 2 is finally found to ben_s The number of points of intersection of the incident ray and the reflected ray with the mirror2 isn_b Then the shadow blocking efficiency of the fixed-sun mirror is.

$$\eta_{sb} = 1 - \frac{n_S+n_B}{n_p} \tag{21}$$

(6) Calculating the optical efficiency of each heliostat at each time point from (10).

(7) Calculate the output thermal power of the heliostat field from (4)-(8).

ISSN 2616-5775 Vol. 7, Issue 5: 229-235, DOI: 10.25236/AJCIS.2024.070530

The efficiency of a single heliostat is shown in Figure 2.

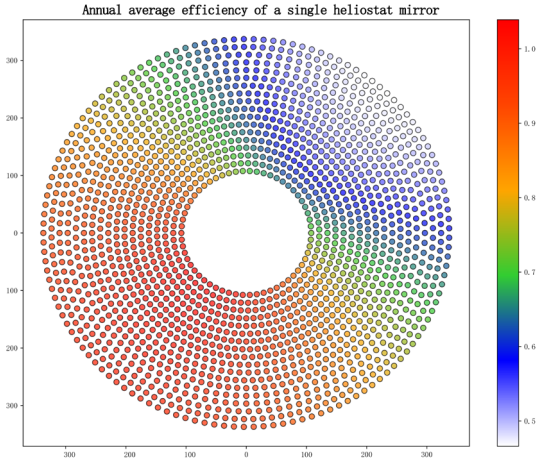

Figure 2: Cloud of annual average efficiency of a single heliostat mirror

Since the site was selected in the northern hemisphere, the average annual thermal efficiency cloud for each heliostat is more realistic. The calculated efficiency and thermal power are shown in Figure 3.

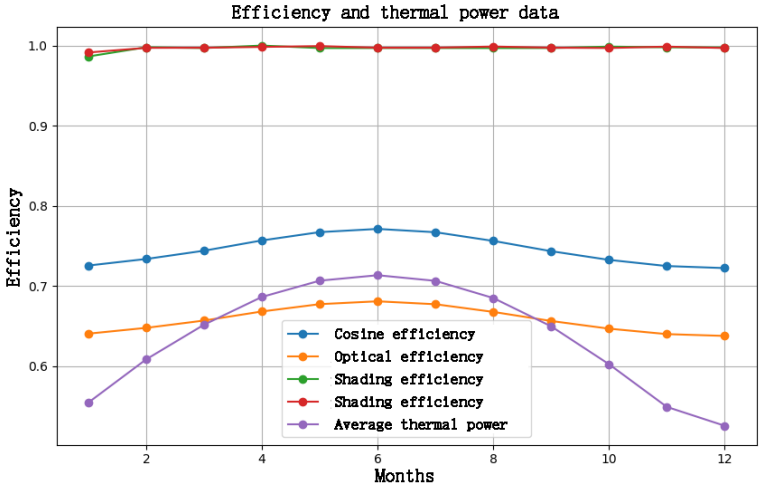

Figure 3: Efficiency and thermal power graph

3. Design of the heliostat field

3.1 Modeling

Firstly, we need to set the annual average output thermal power of the fixed-sun mirror field to 60 MW, and at the same time, we need to ensure that the annual average output thermal power per unit mirror area is as large as possible, and considering other constraints, we have established a constrained multi-objective parameter optimization model as follows.

$$\max L = \frac{\sum_{a=1}^{12}\sum_{b=1}^{5}\left[DNI_{ab}\sum_{i=1}^{N}A_i\eta_{ab}\right]}{N \cdot A} \tag{22}$$

ISSN 2616-5775 Vol. 7, Issue 5: 229-235, DOI: 10.25236/AJCIS.2024.070530

$$s.t.\begin{cases} 2 \le l_H \le 8 \\ 2 \le l_w \le 8 \\ 2 \le h \le 6 \\ \frac{l_H}{2} < h \\ \sum_{a=1}^{12}\sum_{b=1}^{5}[DNI_{ab}\sum_{i=1}^{N}A_i\,\eta_{ab}] = 60 \\ \Delta S_{i,1} = \Delta S_{i,2} = \cdots = kl_w \\ \Delta R_{ij} = \sqrt{c^2 - \left(S_{i,j/2}\right)^2} \end{cases} \tag{23}$$

Where l_H is the height of the heliostat, and l_w is the width of the heliostat. H is the mounting height of the heliostat, and A_i is the area of the $i-$th heliostat.

Due to the excessive number of variables, it is very difficult to optimize the solution directly, so we get the arrangement of the fixed heliostat mirror field by searching the literature, which is mainly divided into: Campo arrangement, DELSOL layout, EB layout, etc. [4-5]. In this paper, we only discuss the Campo arrangement and the EB arrangement.

(1) Campo arrangement in this arrangement, if the heliostats are arranged in the densest way, the positional relationship of the heliostats is shown in Figure 4.

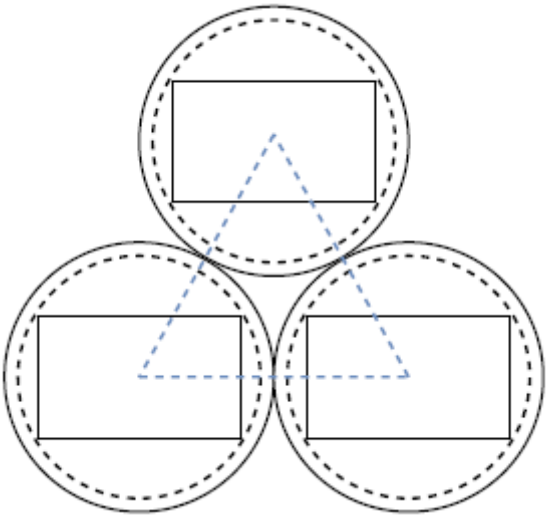

Figure 4: Positional relationship of the heliostat

Since this arrangement of heliostats makes the azimuth and spacing between the heliostats very small, it may result in extensive loss of shadow obscuration, so this arrangement is not chosen in this paper.

(2) EB Arrangement The schematic diagram of the EB arrangement is shown in Figure 5.

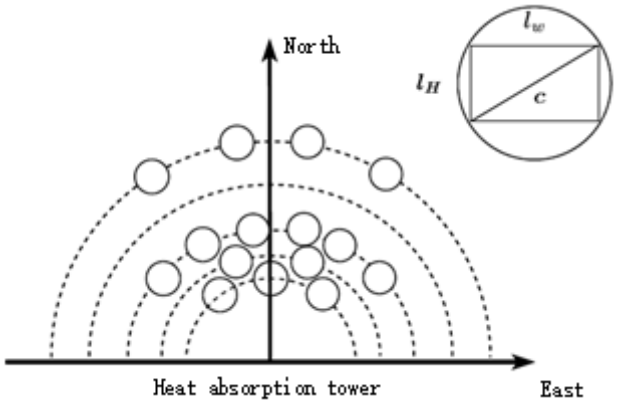

Figure 5: Positional relationship of the heliostat

The azimuthal spacing of the regional heliostats in the mirror field is:

ISSN 2616-5775 Vol. 7, Issue 5: 229-235, DOI: 10.25236/AJCIS.2024.070530

$$\Delta S_{i,1} = \Delta S_{i,2} = \cdots = kl_w \tag{24}$$

Where k is the azimuthal spacing factor, which is mainly related to the tower height and is usually taken as 2.

The radial spacing between neighboring mirror fields is:

$$\Delta R_{ij} = \sqrt{c^2 - \left(S_{i,j/2}\right)^2} \tag{25}$$

3.2 Particle swarm algorithm

The particle swarm optimization algorithm proceeds as follows [6].

Step 1: Initialize the particle swarm parameters c1 and c2, set the position boundary range and velocity boundary range, initialize the particle swarm, and initialize the particle swarm velocity.

Step 2: Calculate the fitness value according to the fitness function and record the historical optimal value p_{best} and the global optimal value g_{best} The global optimal value is recorded.

Step 3: Utilizing the velocity update formula.

$$v_{ij}(t+1) = v_{ij}(t) + c_1 r_1 \left(p_{bestij}(t) - x_{ij}(t)\right) + c_2 r_2 \left(g_{bestj} - x_{ij}(t)\right) \tag{26}$$

The velocity of the particle swarm is updated and bounded for out-of-bounds velocities.

Step 4: Utilize the position update formula $x_{ij}(t+1) = x_{ij}(t) + v_{ij}(t+1)$ Update the position of the particle swarm and constrain the out-of-bounds position.

Step 5: Calculate the fitness value based on the fitness function.

Step 6: For each particle, compare its fitness value with its historical optimal fitness value and if it is better, it will be taken as the historical optimal value p_{best} .

Step 7: For each particle, compare its fitness value with the fitness value of the optimal position experienced by the population, and if better, use it as the global optimum p_{best} .

Step 8: Determine whether the end condition is reached (the maximum number of generation times is reached), if so, output the optimal position, otherwise repeat steps 3-8.

Parameters and the predicted or empirical system efficiencies can estimate the number of heliostats for the entire mirror field.

$$N = \frac{P_e \cdot SM}{DNI \cdot S_{\text{helio}} \cdot \eta_{\text{helio}} \cdot \eta_r} \tag{27}$$

The partial results obtained from the calculations are shown in Table. 1.

Table 1: Results

Optic efficiency	Cosine efficiency	Shadow efficiency	Truncation efficiency	Output thermal power	Output thermal power per unit
0.704023	0.846548	0.992764	0.940444	60.469986	1.291777

4. Optimization of heliostat field design

To further limit the size of the heliostat, the mounting height can be different, we adjust the constraints of the model based on the assumptions in the previous section and some parameter selections and solve the model using the particle swarm algorithm to get the final results.

$$\max L = \frac{\sum_{a=1}^{12} \sum_{b=1}^{5} \left[DNI_{ab} \sum_{i=1}^{N} A_i \eta_{ab} \right]}{\sum \cdot A} \tag{28}$$

ISSN 2616-5775 Vol. 7, Issue 5: 229-235, DOI: 10.25236/AJCIS.2024.070530

$$s.t.\begin{cases} 2 \le l_H \le 8 \\ 2 \le l_w \le 8 \\ 2 \le h \le 6 \\ \frac{l_H}{2} < h \\ \sum_{a=1}^{12}\sum_{b=1}^{5}[DNI_{ab}\sum_{i=1}^{N}A_i\,\eta_{ab}] = 60 \\ \Delta S_{i,1} = \Delta S_{i,2} = \cdots = kl_w \\ \Delta R_{ij} = \sqrt{c^2 - \left(S_{i,j/2}\right)^2} \end{cases} \tag{29}$$

The results of the solution are shown in Table. 2 below.

Table 2: Results

Optic efficiency	Cosine efficiency	Shadow efficiency	Truncation efficiency	Output thermal power	Output thermal power per unit
0.698936	0.829881	0.993797	0.960444	70.179504	1.208542

5. Conclusions

In this study, we have successfully improved the energy utilization efficiency of a photovoltaic power plant by optimizing the design of a circular heliostat field. Through the application of Monte Carlo simulation and particle swarm algorithm, we effectively optimized the size, mounting height, and other parameters of the heliostat mirror to maximize the optical efficiency and thermal power output. Our results show that the annual average output power per unit mirror area of the heliostat field is significantly improved while keeping the rated annual output power constant, which provides an important guidance for new energy applications and the realization of carbon emission reduction targets. This study contributes to the promotion of carbon emission reduction efforts and sustainable development in China and provides useful insights for the design and optimization of future photovoltaic power plants.

References

[1] He J, Li Z, Zhang X, et al. Comprehensive report on China's long-term low-carbon development strategies and pathways[J]. Chinese Journal of Population, Resources and Environment, 2020, 18(4): 263-295.

[2] Awan A B, Zubair M, Mouli K V V C. Design, optimization and performance comparison of solar tower and photovoltaic power plants[J]. Energy, 2020, 199: 117450.

[3] Jeong M, Hammig M D. Comparison of gamma ray localization using system matrixes obtained by either MCNP simulations or ray-driven calculations for a coded-aperture imaging system[J]. Nuclear Instruments and Methods in Physics Research Section A: Accelerators, Spectrometers, Detectors and Associated Equipment, 2020, 954: 161353.

[4] Rizvi A A, Danish S N, El-Leathy A, et al. A review and classification of layouts and optimization techniques used in design of heliostat fields in solar central receiver systems[J]. Solar Energy, 2021, 218: 296-311.

[5] Belaid A, Filali A, Hassani S, et al. Heliostat field optimization and comparisons between biomimetic spiral and radial-staggered layouts for different heliostat shapes[J]. Solar Energy, 2022, 238: 162-177.

[6] Ali M M, Kaelo P. Improved particle swarm algorithms for global optimization[J]. Applied mathematics and computation, 2008, 196(2): 578-593.